energies

MDPI

Article

Compatibility of Methanol-Hydrotreated Vegetable Oil Blends with Chosen Steels and Aluminum

Huaying Wang-Alho *, Katriina Sirviö, Carolin Nuortila, Jonna Kaivosoja, Maciej Mikulski and Seppo Niemi

School of Technology and Innovations, University of Vaasa, 65101 Vaasa, Finland; katriina.sirvio@uwasa.fi (K.S.); carolin.nuortila@uwasa.fi (C.N.); jonna.kaivosoja@uwasa.fi (J.K.); maciej.mikulski@uwasa.fi (M.M.); seppo.niemi@uwasa.fi (S.N.)

* Correspondence: huaying.wang-alho@uwasa.fi; Tel.: +358-29-449-8782

Abstract: Methanol and hydrotreated vegetable oil (HVO) are complementary in the context of achieving ultra-low emission levels via low temperature combustion. HVO is a high-quality fuel fully compatible with compression ignition engines. Standalone methanol combustion is relatively straight-forward according to the Otto principle, with a spark ignited or in conventional dual-fuel ("liquid spark") engines. These two fuels have by far the largest reactivity span amongst commercially available alternatives, allowing to secure controllable partially premixed compression ignition with methanol–HVO emulsification. This study investigates the corrosion of aluminum, carbon steel, stainless steel, and a special alloy of MoC210M/25CrMo4+SH, exposed to different combinations of HVO, HVO without additives (HVOr), methanol, and emulsion stabilizing additives (1-octanol or 1-dodecanol). General corrosive properties are well determined for all these surrogates individually, but their mutual interactions have not been researched in the context of relevant engine components. The experimental research involved immersion of metal samples into the fuels at room temperature for a duration of 60 days. The surfaces of the metals were inspected visually and the dissolution of the metals into fuels was evaluated by analyzing the fuels' trace metal concentrations before and after the immersion test. Furthermore, this study compared the alterations in the chemical and physical properties of the fuels, such as density, kinematic viscosity, and distillation properties, due to possible corrosion products. Based on these results, methanol as 100% fuel or as blending component slightly increases the corrosion risk. Methanol had slight dissolving effect on aluminum (dissolving Al) and carbon steel (dissolving Zn). HVO, HVOr, and methanol–HVOr–co-solvents were compatible with the metals. No fuels induced visible corrosion on the metals' surfaces. If corrosion products were formed in the fuel samples, they did not affect fuel parameters.

Keywords: renewable fuels; fuel blending; co-solvents; corrosion; material compatibility

Citation: Wang-Alho, H.; Sirviö, K.; Nuortila, C.; Kaivosoja, J.; Mikulski, M.; Niemi, S. Compatibility of Methanol-Hydrotreated Vegetable Oil Blends with Chosen Steels and Aluminum. *Energies* **2024**, *17*, 3423. https://doi.org/10.3390/en17143423

Academic Editor: Adam Smoliński

Received: 7 June 2024
Revised: 5 July 2024
Accepted: 9 July 2024
Published: 11 July 2024

1. Introduction

The twin issues of scarcity of oil resources and environmental pollution are very real problems. The transportation sector is heavily dependent on fossil hydrocarbons, which has significant implications for both global warming and local air quality [1]. Conventional compression ignition (CI) engines currently account for approximately half of the greenhouse gas emissions from global transportation. Diesel engines also have the additional challenge of their inherent trade-off between NOx and soot particle emissions. Researchers have strived to address the shortcomings of traditional diesel engines by exploring alternative fuels and advanced combustion modes [2–5].

Methanol is one of the alternative fuels. As a renewable energy source, it plays a pivotal role in reducing global dependence on fossil energy, thus mitigating the effects of global warming and ensuring energy security [6]. Methanol is regarded as a potential carbon-neutral fuel and energy carrier for the future. It can be synthesized entirely from renewable resources via two primary pathways. First is the thermochemical pathway, in

which biomass is gasified into synthesis gas under favorable thermodynamic conditions. The second pathway is biochemical, involving the anaerobic digestion of biomass by microbes to produce methane biogas [7]. In future, methanol can be produced 100% renewably, for example utilizing renewable hydrogen and captured CO_2 [8]. Methanol is considered a promising candidate fuel for decarbonizing marine engines [9]. Additionally, hydrotreated vegetable oil (HVO) renewable diesel is made from renewable raw materials such as used cooking oil, animal fat from food industry waste, or crude tall oil, a residue of pulp production. In certain CI engines, HVO exhibits lower greenhouse gas (GHG) emissions throughout its life cycle compared to fossil diesel. Furthermore, good-quality HVO is compatible with all CI engines [10–12].

Methanol exhibits desirable characteristics, including a high stoichiometric fuel-to-air ratio, high oxygen content, high hydrogen-to-carbon ratio, and a significant latent heat of evaporation, enabling a wide engine–load range. These contribute to the reduction in NOx emissions and soot [13,14]. However, these properties necessitate a highly reactive fuel to facilitate controlled self-ignition in low-temperature combustion (LTC) conditions. HVO's chemical structure offers favorable characteristics in terms of auto-ignition properties and in enabling clean combustion. HVO is considered one of the most reactive renewable alternatives, and its clean paraffinic structure helps to mitigate the formation of particulate matter [10,15]. Importantly, emulsification in the pre-blending of methanol and HVO can address methanol's lubricity issues. It is noteworthy that blending methanol and HVO fuel does not result in a stable, single-phase fuel. However, the addition of co-solvents such as 1-octanol and 1-dodecanol in the blending does enable production of a stable single-phase fuel [16].

Corrosion of metallic materials in the presence of alternative fuels has become an important concern in various industries, including automotive and marine applications [17]. Methanol, HVO, and their blends are emerging as potential fuel alternatives due to their renewable nature and reduced environmental impact, as well as their blending properties for LTC concepts [18]. However, the compatibility of these fuels with different metal alloys used in engine components is not yet fully clear.

The use of methanol can cause corrosion of engine components [19]. There are three primary types of corrosion induced by alcohols: general corrosion, dry corrosion, and wet corrosion. General corrosion arises from ionic impurities such as chloride ions and acetic acid. Dry corrosion is attributed to the polarity of the alcohol molecule. Wet corrosion ensues from the azeotropic formation of alcohol and water [20]. Alcohols' corrosive properties stem from the increased conductivity from their polar hydroxyl groups. Corrosion tendencies are further increased when the fuel has additional polar impurities, including water, absorbed atmospheric oxygen, sulfur, and ions, as well as various acids or bases [21]. The strong attraction of methanol to water makes it probable that water will enter during transportation and formic acid will be generated. This will activate the acidic corrosion and electrochemical corrosion of metals. Methanol is corrosive to many metals in the engine fuel system, such as stainless steel, copper, brass, aluminum, or carbon steel [19,22].

HVO is a second-generation bio-sourced fuel for CI engines. The hydrotreating process used during HVO production eliminates heteroatoms (typically oxygen, nitrogen, and sulfur) from organic feedstock to obtain hydrocarbons, and reduces the presence of reactive compounds that could potentially induce corrosion [5]. Although use of HVO–methanol blends in CI engines is gaining attention, there remains a notable dearth of research focused on thoroughly investigating the effects of these blends on the materials found in CI engines. The tendency for phase separation in methanol–HVO fuel blends [18], primarily due to methanol's affinity for water, is a particular concern for potential corrosion in engine components. Addition of co-solvents, 1-octanol and 1-dodecanol, mitigates the phase separation issues [16]. However, the effect that these co-solvents may have on material compatibility also needs to be better understood.

Both 1-octanol and 1-dodecanol are higher alcohols, capable of serving as co-solvents and alternative fuels for engines [23,24]. The term 'higher alcohol' usually refers to the

series of straight-chain alcohols containing four or more carbon atoms. Higher alcohols are less corrosive, have a higher energy density, a higher cetane number, a better blend stability, and are less hygroscopic compared to methanol. Since they are less hygroscopic, higher alcohols can be less corrosive on materials used in fuel delivery and injection systems [20,25].

Fuels are exposed to metallic and non-metallic elements in engine components. Fuel systems are made of ferrous materials such as steel and cast iron, and non-ferrous materials such as aluminum and copper alloys [26]. Fuel tanks, fuel supply pumps, fuel lines, pumps, injectors, nozzles, and valves are mostly made of steel and stainless steel. Pistons are usually made of steel and nodular cast iron. Cylinder liners are made of grey cast iron or cast aluminum [27]. Piston pins are commonly made of carbon steel and alloy steel [28].

Trace elements in the fuel can have detrimental effects on both the fuel intake system, including nozzles and valves, and the exhaust system. Trace elements can also lead to catalyst deactivation. Furthermore, the presence of trace elements contributes to the formation of ash during the combustion process, which again can cause deposit formation and filter plugging. These trace element metals can include vanadium (V), sodium (Na), iron (Fe), silicon (Si), calcium (Ca), magnesium (Mg), aluminum (Al), and nickel (Ni). Among these, V and Na are particularly problematic as they can contribute to hot corrosion in engine components. Additionally, alkaline metals, such as Na and K, can have adverse effects on aftertreatment systems used for emission abatement [29]. The World Fuel Charter (WFC) addresses these concerns with guidelines specifying that the total concentration of trace elements in diesel fuel should not exceed 1 ppm. These guidelines cover a range of restricted elements, including metallic elements such as copper (Cu), Fe, manganese (Mn), Na, lead (Pb), and zinc (Zn); semi-metallic elements such as silicon (Si); and non-metallic elements such as phosphorus (P), sulfur (S), and chlorine (Cl). It is important to note that these recommendations are applicable globally, regardless of local fuel requirements [30].

HVO is said to be 100% compatible with engines but there is a lack of extensive research on the compatibility of methanol–HVO blends, methanol–HVO blends with added co-solvents, and HVO fuel with the metals commonly used in the fuel system of CI engines. Some studies have investigated the corrosion mechanisms of metals in methanol, but a comprehensive analysis of methanol's corrosion and compatibility with materials used in engine components is still needed.

This study aimed to examine and compare the impact of possible corrosion on the physical and chemical properties of the fuels. Corrosion products can alter important fuel characteristics such as density, kinematic viscosity, and distillation properties. These changes can subsequently affect engine performance and efficiency. We aimed to gain a better understanding of the fuels' behavior in the presence of different metal alloys by analyzing the changes. The present study used the immersion test method to investigate the corrosion of aluminum, carbon steel, stainless steel, and a special alloy of MoC210M/25CrMo4+SH. They were exposed to methanol, HVO, HVO without additives (HVOr), a methanol–HVO blend (MeOH50), and methanol–HVOr blends with added co-solvents (MeOH50-1-octanol and MeOH50-1-dodecanol). These materials were chosen because they come into contact with the fuel as it passes from the tank to the combustion chamber [26].

2. Materials and Methods

2.1. Materials

The six fuels studied in this research were (1) methanol (later MeOH), (2) HVO, (3) a 50/50% mixture of methanol and HVO (later MeOH50), (4) HVO without additives (later HVOr), (5) a 50/50% mixture of methanol and HVOr with co-solvent 1-octanol added (later MeOH50-O, and (6) a 50/50% mixture of methanol and HVOr with co-solvent 1-dedocanol added (later MeOH50-D). The MeOH–HVO blends shares were calculated based on the energy density. The lower heating values (LHV) used for the calculations were 44 MJ/kg for HVO and HVOr [31] and 20 MJ/kg for methanol [32]. The co-solvents were added just to

the amount required to form a stable single-phase liquid. The quantities of 1-octanol, 1-dodecanol, and methyl butyrate in 250 mL of the MeOH50–co-solvent mixture are 66.8 mL, 53.9 mL, and 96.6 mL, respectively. Methanol was a product of Merck KGaA, analysis grade, purchased from VWR, Helsinki, Finland. HVO was Neste MY renewable diesel, purchased from a Neste filling station in Vaasa, Finland. HVOr was Neste MY renewable diesel without additives supplied by Neste, Finland.

According to the manufacturers' data, methanol and HVO exhibited metal contents (Al, Cu, Fe, Mn, V, Zn, and Pb) of less than 1 ppm and a water content of less than 500 ppm.

The metals were purchased in the form of rods from a hardware store, Hartman Rauta Oy, in Vaasa, Finland. They included carbon steel (CS; grade Imatra 550), stainless steel (SS; 1.4301/1.4307), a special alloy steel known as MoC210M/25CrMo4+SH (CrMo), and aluminum EN AW-6082 alloy of high strength and good corrosion resistance. Ingredient certificates for the rods were provided.

Table 1 lists the concentrations of the studied metals in the steels and aluminum alloy. The ingredient certificates for the steels did not give the concentrations of Al, Zn, and Fe. These elements were later analyzed from the fuels, along with Cu, Mn, Si, V, Zn, and Pb. The amount of Fe was above 70% according to the literature for the three steels [33].

Table 1. The concentration of the elements in the metals.

	Carbon Steel	Stainless Steel	MoC210M/25CrMo4+SH	Aluminum EN AW-6082 Alloy
Cu (%)	0.20	0.96	0.20	0.01
Fe (%)	>70	>70	>70	0.20
Mn (%)	1.13	1.66	0.81	0.41
Si (%)	0.24	0.27	0.27	1.07
V (%)	0.06		0.01	
Pb (%)	0.0003		0.0007	<0.05
C (%)	0.13	0.023	0.27	
Cr (%)	0.20	18.10	0.99	0.13
Ni (%)	0.15	8.01	0.19	
Mo (%)	0.03	0.29	0.22	
Mg (%)				0.70
Zn (%)				0.01
Ti (%)				0.02

2.2. Methods

Experimental studies were performed to evaluate the compatibility of the selected materials and methanol, HVO, and their 50:50 blend, as well as the 50:50 blends stabilized with co-solvents. The metal bars were immersed in the fuel samples. The samples were kept in a fume cupboard at room temperature for 60 days. The surfaces of the metals were inspected visually at the end of this period, and the dissolution of the metals into fuels was evaluated by analyzing the fuels' trace metal concentrations before and after the immersion test. The trace elements were analyzed using an inductively coupled plasma optical emission spectroscope (ICP-OES). This evaluates the presence and concentration of the elements by comparing the intensity of light wavelength emissions to those emitted by known concentrations of various elements. The concentrations of metal elements (Al, Cu, Fe, Mn, Si, V, Zn, and Pb) were determined for all the fuel samples. This study aimed to investigate if the trace metals had dissolved from the rods during the immersion test.

Each of the six different fuel samples (MeOH, HVO, HVOr, MeOH50, MeOH50-O, and MeOH50-D) amounted to 250 mL and was transferred into borosilicate glass bottles. In total, 24 samples were prepared (Table 2, Figure 1), with each paired with a round rod made of one of three types of steel and aluminum alloys. The rods were 10 cm long and 2 cm in diameter. Each rod was completely immersed in the liquid fuel and each bottle was closed with a polypropylene screw cap. In MeOH50 samples without co-solvent, the fuels separated into two phases; due to its higher density, methanol formed the lower phase.

Therefore, the metals mainly were in the MeOH layer during the test. The methanol–HVOr fuels stabilized with co-solvents stayed in one phase during the 60-day immersion period. The corrosion on the surface of the metal rods was assessed visually, before and at the end of the 60-day immersion period.

Table 2. Prepared samples.

Sample Matrix (Fuel/Metal)	Carbon Steel	Stainless Steel	MoC210M/25CrMo4+SH	Aluminum
MeOH	MeOH CS	MeOH SS	MeOH CrMo	MeOH Al
HVO	HVO CS	HVO SS	HVO CrMo	HVO Al
MeOH50	MeOH50 CS	MeOH50 SS	MeOH50 CrMo	MeOH50 Al
HVOr	HVOr CS	HVOr SS	HVOr CrMo	HVOr Al
MeOH50-O	MeOH50-O CS	MeOH50-O SS	MeOH50-O CrMo	MeOH50-O Al
MeOH50-D	MeOH50-D CS	MeOH50-D SS	MeOH50-D CrMo	MeOH50-D Al

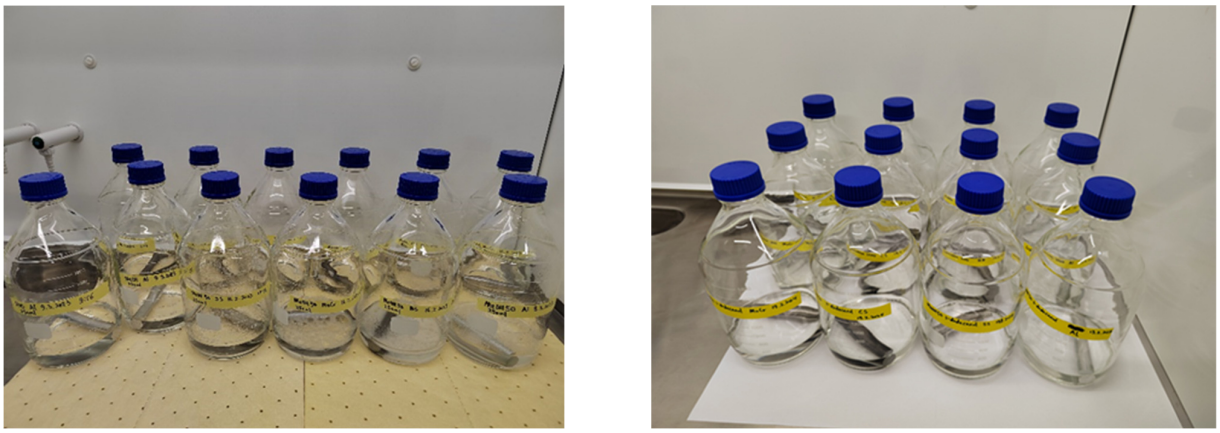

(**a**) (**b**)

Figure 1. The samples were stored in a fume cupboard at room temperature: (**a**) The fuels are methanol, HVO, and MeOH50; (**b**) the fuels are HVOr (without additives) and fuel blends of MeOH50 with co-solvents 1-octanol and 1-dodecanol added. The metal rods in the fuels are carbon steel, stainless steel, MoC210M/25CrMo4+SH, and aluminum.

2.2.1. Determination of Trace Metals

The metal concentrations in the fuel samples were analyzed before and after the metal immersion test. The immersion tests were conducted in two series. In the first, the samples were methanol, HVO, and the MeOH50 blend. The methanol and HVO had separated into two different phases in the MeOH50 blend. Therefore, the analyses of trace metals after immersion in MeOH50 fuel were performed in the methanol part of the blend separately from the HVO part of the blend. The samples in the second immersion series were HVOr, MeOH50-O, and MeOH50-D.

In the first measurement series, weighed HVO samples were diluted with kerosene in a weight ratio of 1:1 and then injected into the spectrometer plasma. The concentrations of metal elements (Al, Cu, Fe, Mn, Si, V, Zn, and Pb) were determined using a PerkinElmer 7000 DV ICP-OES instrument. The analyses followed an in-house method based on Standards EN 14538 and EN 14107 [34,35], in accordance with the advice of the spectrometer's manufacturer. The determination limit was 1 ppm for all elements. Pre-treatment of the samples prior to trace element analysis differed for the methanol and MeOH50 samples in the first test series and in the second measurement series.

The analysis procedure for methanol and MeOH50 samples in the first test series included pre-treatment by a method using closed-cup microwaves to assist acid digestion to decompose all the inorganic particles of less than ~8 µm size and to destroy the remains of organic matrices. After acid digestion, the samples were diluted and analyzed by an

ICP-OES (Thermo Scientific iCAP 6500 Duo). The concentrations of metal elements (Al, Cu, Fe, Mn, Si, V, Zn, and Pb) were determined. The analyses were conducted following an in-house method.

The analysis procedure for HVOr and MeOH50-co-solvent samples in the second measurement set included a pre-treatment using a microwave oven (MARS 6 iWave by CEM) to assist acid digestion to decompose all the inorganic particles of less than ~8 µm size and to destroy the remains of organic matrices. After microwave-assisted digestion with nitric acid, the samples were diluted and analyzed by an ICP-OES PerkinElmer Avio 500. The concentrations of elements (Al, Cu, Fe, Mn, Si, V, Zn, and Pb) were determined. The analyses were conducted following an in-house method. The determination limit was 1 ppm for elements Al, Cu, Fe, Si, V, and Zn; 2 ppm for Mn; and 4 ppm for Pb.

2.2.2. Analysis of Fuel Properties

The physical and chemical properties of the fuels were analyzed before and after immersion of the metal rods. The MeOH50 samples (without co-solvents) were mixed thoroughly before the analyses to form an emulsion. Nevertheless, these samples tended to separate into two phases during the measurements. Conversely, MeOH50-1-octanol and MeOH50-1-dodecanol formed stable, single-phase fuel mixtures.

Analyses included density, kinematic viscosity, and distillation properties, such as distillation curve, initial boiling point, IBP, and final boiling point, FBP. The density and the kinematic viscosity were measured with an SVM 3000 viscometer, and the measurement was produced according to Standard ASTM D7042 [36]. The measurement is based on torque and speed measurements, with the device calculating dynamic viscosity from the rotor speed. It also has a density-measuring cell that employs an oscillating U-tube principle. The kinematic viscosity is calculated automatically from these measurements. The reproducibility of the SVM 3000 viscometer is −0.04% for density and 0.06% for viscosity [37].

Distillation properties were measured using OptiPMD Automatic Distillation equipment, and the measurement was produced according to Standard ASTM D7345 [38]. The obtained distillation curve shows the transition from liquid to vapor with respect to temperature. The reproducibility for the OptiPMD Automatic Distillation equipment is not known [39].

The obtained results were average values of at least two measurements. The relative standard deviations for the analysis methods had been measured earlier, and they were the following: kinematic viscosity < 1.0%; density < 1.0%; IBP < 1.1%; and FBP < 1.1%.

3. Results

3.1. Visual Evaluation of Metal Corrosion

A visual evaluation of corrosion was performed for all the metal samples before and after the immersion test. No signs of corrosion were observed on any of the metal bars.

3.2. Concentration of Trace Metals in Exposed Fuel Samples

Table 3 shows the concentrations of trace metals in all fuel samples after the immersion. The concentrations of Al, Cu, Fe, V, and Zn were below or 1 ppm in most of the samples. Two exceptions to this were the MeOH Al sample, which had an Al concentration of 2 ppm, and the MeOH CS sample, with a Zn concentration of 2 ppm.

The HVO CS sample had a Si content of less than 2 ppm. MeOH CS, MeOH SS, MeOH CrMo, and MeOH Al showed Si contents of 3 ppm. Si contents in MeOH50 CS and MeOH50 SS fuels were 5 ppm. MeOH50 CrMo and MeOH50 Al had Si concentrations of 3 ppm. The Si contents in other samples were below 1 ppm. However, according to Joo and Suh, determining Si accurately in a sample using ICP-OES is difficult as SiO_2 from the ICP spectrometer's torch may contaminate the samples [40]. This suggests that the Si results need to be evaluated critically.

Table 3. The concentrations of trace metals in all fuel samples. The determination limit was 2 ppm for Mn and 4 ppm for Pb in the HVOr and MeOH–HVOr–co-solvent samples. The determination limit was 1 ppm for all other elements and fuel blends.

Sample	Al ppm	Cu ppm	Fe ppm	Mn ppm	Pb ppm	Si ppm	V ppm	Zn ppm
HVO	<1	<1	<1	<1	<1	<1	<1	<1
HVO CS	<1	<1	<1	<1	<1	< 2	<1	<1
HVO SS	<1	<1	<1	<1	<1	<1	<1	<1
HVO CrMo	<1	<1	<1	<1	<1	<1	<1	<1
HVO Al	<1	<1	<1	<1	<1	<1	<1	<1
MeOH CS	<1	<1	<1	<1	<1	3	<1	2
MeOH SS	<1	<1	<1	<1	<1	3	<1	<1
MeOH CrMo	<1	<1	<1	<1	<1	3	<1	<1
MeOH Al	2	<1	<1	<1	<1	3	<1	<1
MeOH50 CS	<1	1	<1	<1	<1	5	<1	1
MeOH50 SS	<1	<1	<1	<1	<1	5	<1	<1
MeOH50 CrMo	<1	<1	<1	<1	<1	3	<1	1
MeOH50 Al	<1	<1	<1	<1	<1	3	<1	<1
HVOr	<1	<1	<1	<2	<4	<1	<1	<1
HVOr CS	<1	<1	<1	<2	<4	<1	<1	<1
HVOr SS	<1	<1	<1	<2	<4	<1	<1	<1
HVOr CrMo	<1	<1	<1	<2	<4	<1	<1	<1
HVOr Al	<1	<1	<1	<2	<4	<1	<1	<1
MeOH50-O	<1	<1	<1	<2	<4	<1	<1	<1
MeOH50-O CS	<1	<1	<1	<2	<4	<1	<1	<1
MeOH50-O SS	<1	<1	<1	<2	<4	<1	<1	<1
MeOH50-O CrMo	<1	<1	<1	<2	<4	<1	<1	<1
MeOH50-O Al	<1	<1	<1	<2	<4	<1	<1	<1
MeOH50-D	<1	<1	<1	<2	<4	<1	<1	<1
MeOH50-D CS	<1	<1	<1	<2	<4	<1	<1	<1
MeOH50-D SS	<1	<1	<1	<2	<4	<1	<1	<1
MeOH50-D CrMo	<1	<1	<1	<2	<4	<1	<1	<1
MeOH50-D Al	<1	<1	<1	<2	<4	<1	<1	<1

The trace metal concentrations in MeOH50-O, MeOH50-D, and HVOr fuels remained unchanged. The results were below the determination limit (Table 3) in all samples before and after metal immersion. Mn content in all MeOH50-O, MeOH50-D, and HVOr fuels was measured to be below 2 ppm; Pb content was below 4 ppm; and other metal contents (Al, Cu, Fe, Si, V, Zn) were below 1 ppm. The determination limit for Mn and Pb was different in the two measurement series with HVO and HVOr samples. All the trace element contents for HVO and HVOr samples were below the methods' determination limits, which were <2 ppm for Mn; <4 ppm or Pb; and <1 ppm for all other elements.

Notably, the fuel's metal content did not increase after immersing metal bars in HVO fuel for a duration of 60 days, except for the Si content in the HVO CS sample, which rose from 1 ppm to 2 ppm. In MeOH50 samples, the only element showing results above 1 ppm was Si. It can be stated that the MeOH50 samples did not leach metals from CS, SS, CrMo, or Al. However, the 100% MeOH samples showed different results, with Si in all MeOH rising to 3 ppm. Also, it seemed that MeOH leached Al (2 ppm after the immersion), but HVO, HVOr, and the HVO–MeOH blend did not—their Al concentrations remained below 1 ppm after the immersion. In addition, the Zn content had increased from 1 ppm to 2 ppm in the MeOH CS sample after the immersion.

3.3. Influence of Trace Elements on Fuel Properties

3.3.1. Density and Kinematic Viscosity

Table 4 presents the results of the fuel properties testing. The results for the samples MeOH, HVO, MeOH50, HVOr, MeOH50-O, and MeOH50-D (i.e., fuel samples without metal rods) show their initial levels before the immersion test. The results for the rest of the samples were measured after the immersion test.

Table 4. The results of the fuel properties tests for density, kinematic viscosity, and initial and final boiling point, with relative standard deviations (RSD) of each analysis method.

Sample	Density (kg/m^3) 15 °C (RSD < 1.0%)	Kinematic Viscosity, (mm^2/s) 40 °C (RSD < 1.0%)	Initial Boiling Point, (°C) (RSD < 1.1%)	Final Boiling Point, (°C) (RSD < 1.1%)
HVO	781	3.14	223	309
HVO CS	781	3.12	223	300
HVO SS	781	3.14	223	301
HVO CrMo	781	3.13	223	300
HVO Al	781	3.14	223	307
MeOH	795	0.55	65	73
MeOH CS	795	0.56	64	69
MeOH SS	795	0.58	64	70
MeOH CrMo	795	0.56	64	69
MeOH Al	795	0.57	65	74
MeOH50	793	1.25	65	244
MeOH50 CS	793	0.85	66	260
MeOH50 SS	794	1.30	66	252
MeOH50 CrMo	794	1.14	n/a	n/a
MeOH50 Al	793	1.04	65	257
HVOr	781	3.06	223	307
HVOr CS	781	3.05	224	309
HVOr SS	781	3.05	222	308
HVOr CrMo	781	3.06	223	309
HVOr Al	781	3.06	222	309
MeOH50-O	798	1.33	68	259
MeOH50-O CS	797	1.31	68	257
MeOH50-O SS	797	1.33	65	256
MeOH50-O CrMo	797	1.35	68	257
MeOH50-O Al	797	1.40	69	259
MeOH50-D	797	1.61	66	244
MeOH50-D CS	797	1.49	66	246
MeOH50-D SS	797	1.45	65	248
MeOH50-D CrMo	797	1.48	64	228
MeOH50-D Al	797	1.58	66	252

n/a: not analyzed.

The densities of HVO and HVOr were the same (781 kg/m^3), and both remained unchanged during metal immersion. The kinematic viscosity of HVO (initial result being 3.14 mm^2/s) and HVOr (initial 3.06 mm^2/s) remained at almost the same level after the metal immersion. The lower kinematic viscosity values of HVOr fuels before and after metal immersion compared to those of HVO fuels were most likely due to the lack of additives in HVOr samples. The difference was approximately 0.07–0.08 mm^2/s. The kinematic viscosities of HVO SS and HVO Al fuels were the same as for the original HVO fuel, at 3.14 mm^2/s. The kinematic viscosities of HVO CS and HVO CrMo were 3.12 mm^2/s and 3.13 mm^2/s, respectively. The kinematic viscosities of HVOr CrMo and HVOr Al fuels were the same as in the original HVOr fuel, at 3.06 mm^2/s. The kinematic viscosities of HVOr CS and HVO SS were both 3.05 mm^2/s.

The density of all the methanol fuel samples remained unchanged at 795 kg/m^3 during metal immersion. After the immersion, the kinematic viscosities of the methanol samples varied slightly, ranging from 0.58 mm^2/s to 0.56 mm^2/s. These values are 0.01 to 0.03 mm^2/s higher than that of the initial methanol fuel (0.55 mm^2/s), so the changes were minor.

There was negligible variation in the density of MeOH50 fuels after the immersion test compared to the initial MeOH50 fuel, with all samples having a density ranging from 793 to 794 kg/m^3. However, a significant change was observed in their kinematic viscosities, particularly in the case of MeOH50 CS, for which the kinematic viscosity was only 0.85 mm^2/s. This equates to a 32% reduction in kinematic viscosity compared to the initial MeOH50 fuel's value of 1.25 mm^2/s. The kinematic viscosities of MeOH50 CrMo (1.14 mm^2/s) and MeOH50 Al (1.04 mm^2/s) fuels exhibited decreases of 8.8% and 16.8%, respectively. Conversely, the kinematic viscosity of MeOH50 SS (1.30 mm^2/s) fuel experienced a slight increase of 4%. All the samples were mixed properly before the measurements, but the MeOH50 samples tended to move into two phases relatively soon after mixing. The variation in kinematic viscosity values is most likely due to the inaccuracy caused by phase separation.

The density of MeOH50-O was initially recorded as 798 kg/m^3, and decreased only marginally to 797 kg/m^3 for all samples after immersion. The kinematic viscosity of MeOH50-O SS was the same as the initial MeOH50-O, remaining at 1.33 mm^2/s. The kinematic viscosities of MeOH50-O CS, MeOH50-O CrMo, and MeOH50-O Al were 1.31 mm^2/s, 1.35 mm^2/s, and 1.40 mm^2/s, respectively.

The density of MeOH50-D exhibited no change post-immersion, maintaining its initial value of 797 kg/m^3 across all samples. However, the post-immersion kinematic viscosities of the MeOH50-D samples were all lower than the fuel´s initial value of 1.61 mm^2/s. Only MeOH50-D Al, recording a viscosity of 1.58 mm^2/s, was relatively close to the initial measurement. MeOH50-D CS, MeOH50-D SS, and MeOH50-D CrMo recorded reduced viscosities below 1.50 mm^2/s, being 1.49 mm^2/s, 1.45 mm^2/s, and 1.48 mm^2/s, respectively.

Table 4 shows that the density and kinematic viscosity of all MeOH50-O and MeOH50-D blends were higher than those of all MeOH50 blends. The density of all MeOH50-O blends and MeOH50-D blends was largely unaffected by immersion, but their kinematic viscosities exhibited a consistent elevation, with MeOH50-D blends displaying approximately 0.2 mm^2/s higher viscosities than MeOH50-O blends.

A comparative analysis of fuel densities and kinematic viscosities pre- and post-immersion of metal rods reveals that fuel densities remained predominantly unchanged. However, slight fluctuations in kinematic viscosity were observed exclusively in MeOH50 blends and MeOH50–co-solvents after the immersion. Of these, MeOH50 CS had the largest fluctuation, with its kinematic viscosity reduced by 0.4 mm^2/s when compared to the initial MeOH50. The viscosity reductions in MeOH50 CrMo and MeOH50 Al were 0.11 mm^2/s and 0.21 mm^2/s, respectively, compared to the initial MeOH50. The viscosity of MeOH50 SS increased by 0.05 mm^2/s. Other fuel types exhibited negligible alterations in kinematic viscosity.

3.3.2. Distillation Curve Analysis

Figure 2 shows that the distillation behavior of HVO and HVOr fuels after the immersion test closely resembled that of the initial HVO and HVOr fuels. All the HVO fuels before and after metal immersion exhibited the same initial boiling point (IBP) of 223 °C. HVOr and HVOr fuels after metal immersion also exhibited values close to the IBP of HVO fuels.

Figure 3 depicts the distillation curves of the methanol samples, and shows that their IBP values remained unchanged during the immersion. The IBP values were 65 °C for MeOH and MeOH Al; and 64 °C for MeOH CS, MeOH SS, and MeOH CrMo. The final boiling point (FBP) values were recorded at 73 °C for MeOH; 69 °C for MeOH CS and MeOH CrMo; 70 °C for MeOH SS; and 74 °C for MeOH Al.

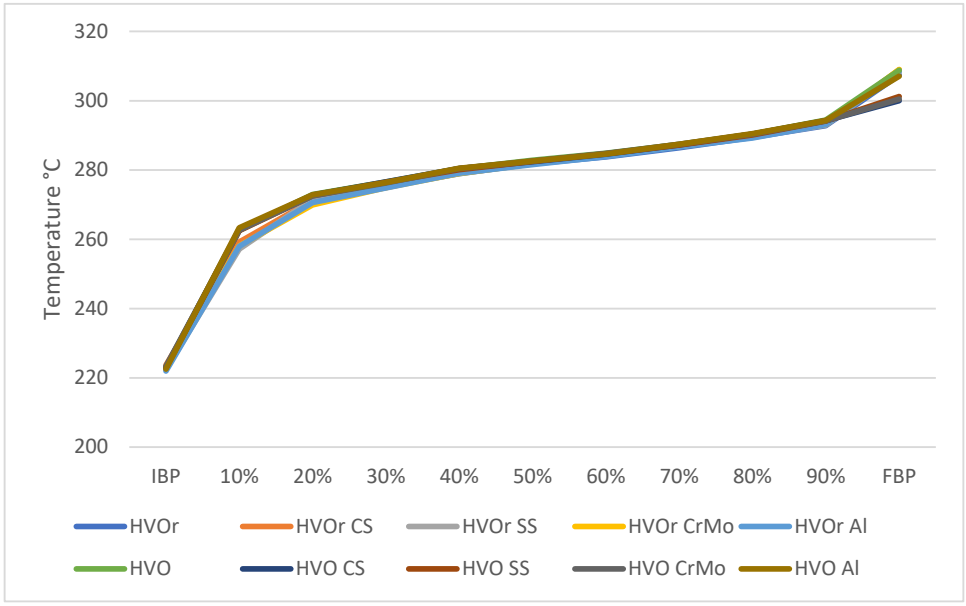

Figure 2. Distillation curves of all the HVO and HVOr samples.

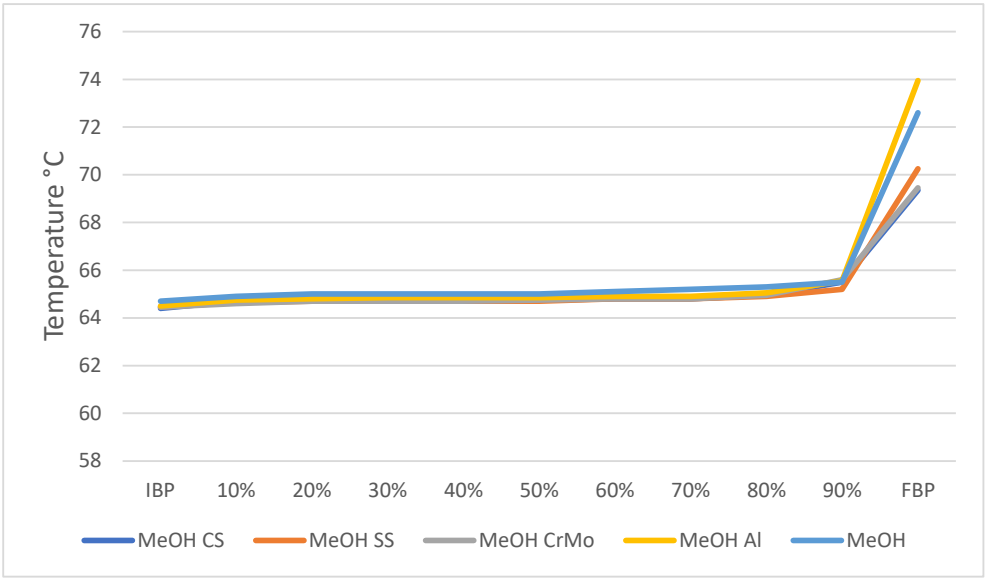

Figure 3. Distillation curves of the samples: MeOH CS, MeOH SS, MeOH CrMo, MeOH Al, and MeOH.

Figure 4 illustrates the distillation curves of all the studied methanol and HVO blends. Notably, throughout the distillation process for all these blends, with the exception of MeOH50 without a metal rod, the equipment reported unstable boiling behavior while measuring the samples.

Table 4 lists the IBP and FBP data for all samples. The IBPs of MeOH50 and MeOH50 Al were both 65 °C, with FBPs of 244 °C and 257 °C, respectively. The IBPs for MeOH50 CS and MeOH50 SS were both 66 °C, and their FBPs were 260 °C and 252 °C, respectively. No results were obtained for the IBP and FBP of MeOH50 CrMo. The IBPs for MeOH50-O, MeOH50-O CS, and MeOH50-O CrMo were all 68 °C, with FBPs of 259 °C, 257 °C, and 257 °C, respectively. The IBPs for MeOH50-O SS and MeOH50-O Al were 65 °C and 69 °C, respectively, with FBPs of 256 °C and 259 °C, respectively. The IBPs for MeOH50-D, MeOH50-D CS, and MeOH50-D Al were all 66 °C, with FBPs of 244 °C, 246 °C, and 252 °C,

respectively. The IBPs for MeOH50-D SS and MeOH50-D CrMo were 65 °C and 64 °C, respectively, with FBPs of 248 °C and 228 °C, respectively.

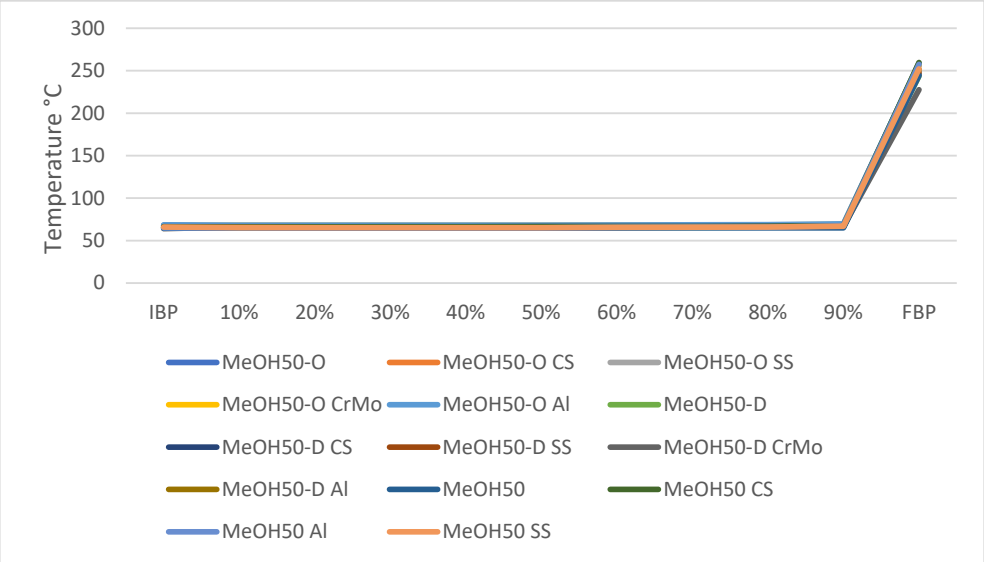

Figure 4. Distillation curves of all the MeOH-HVO blends samples.

Notably, the FBP for MeOH50-D stands at 228 °C. Additionally, Figure 4's distillation curves show that all MeOH50 and MeOH50–co-solvent blends remained largely consistent before and after the metal immersion. It is worth noting that the distillation curve of MeOH50 did not change significantly after adding the co-solvents 1-octanol and 1-dodecanol. Moreover, the distillation behavior for fuels after the metals' immersion was similar to those samples that were analyzed before the immersion.

4. Discussion

This study's findings will aid understanding of the compatibility between various metals and methanol, HVO, and methanol–HVO blends, the latter studied with and without stabilizing co-solvents as additives. Moreover, a better understanding of corrosion behavior and its impact on fuel properties will increase the knowledge of fuel formulation optimization to enhance engine performance and reduce maintenance costs.

4.1. Fuel and Metal Compatibility

The visual assessment of metal corrosion conducted in this study yielded favorable results, with no discernible signs of corrosion observed on the surfaces of aluminum, carbon steel, stainless steel, and the special MoC210M/25CrMo4+SH alloy immersed in any fuel. This lack of conspicuous signs of corrosion suggests the potential compatibility of these metals with methanol, HVO, HVOr, MeOH–HVO, and MeOH–HVO–co-solvent fuels in the studied conditions.

However, the 100% MeOH sample seemed to dissolve Al, resulting in Al content of 2 ppm in the MeOH Al sample after the immersion. Al content in all other fuels and blends was below 1 ppm after immersion. In addition, Zn content increased from 1 ppm to 2 ppm in the MeOH CS sample after the immersion. These increments are minor but the results may indicate that exposing carbon steel and aluminum to methanol may increase the risk of corrosion. The conditions during this experiment were stable, with temperature, for example, at approximately 20 °C. At higher temperatures and exposed to mechanical wear, the results might show greater damage in the studied materials or in the fuel quality.

Measuring the physical–chemical properties of the MeOH50 blend without co-solvents showed that the liquids tended to separate and form an unstable solution. This made it hard or even impossible for the used devices to measure the properties precisely. Most

likely, this behavior caused the variation in the kinematic viscosity results. Better results for the MeOH50 blends required stabilization of the blend. Therefore, this study used 1-octanol and 1-dodecanol as co-solvents to form a stable, single-phase fuel blend of MeOH–HVO.

The density and kinematic viscosity results of the MeOH50 blends are between those measured for neat MeOH and HVO. In a previous study by Wang-Alho et al. [18], the density and kinematic viscosity values of MeOH–HVO blends formed a noticeable trendline between neat HVO and neat methanol, with the increasing amount of MeOH. The current study's kinematic viscosity values observed for MeOH50-O and MeOH50-D fall within the viscosity range exhibited by methanol and HVO, but are higher than those of MeOH50. Notably, the density of MeOH50-O and MeOH50-D exceeds that of methanol, HVO, HVOr, and MeOH50.

The experimental investigation revealed that the density of MeOH50, MeOH50-O, and MeOH50-D blends remained unaltered following exposure to the metals, whereas noteworthy changes were noticed in both kinematic viscosity and FBP. MeOH50 CS fuel exhibited a kinematic viscosity of 0.85 mm^2/s. The kinematic viscosity values for all MeOH50, MeOH50-O, and MeOH50-D, both before and after metal immersion, range between 0.85 mm^2/s and 1.61 mm^2/s. They are, therefore, below the kinematic viscosity threshold of 1.9 mm^2/s at which fuel leakage may occur from the injector nozzle sealing and high-pressure pump system [18,41]. Additionally, the low viscosity of fuel may cause pump wear [42]. Addressing this issue entails the use of advanced hydraulic sealing systems [18,41]. However, as mentioned, the unstable behavior of the HVO–methanol blend may have affected the results if the sample contained more methanol than HVO. The distillation curves obtained for MeOH50, MeOH50 CS, MeOH50 SS, MeOH50 CrMo, and MeOH50 Al fuels exhibited instability during the distillation measurement. Of these, only MeOH50 CrMo did not provide distillation results.

The distillation curves of MeOH50-O before and after the metal immersion were basically the same. Examination of the MeOH50-D curves shows that the IBP of the fuel after immersion remains unchanged, although changes are noted in the FBP. With the exception of MeOH50-D CrMo, where the FBP decreased, a marginal increase was seen in the FBPs of other MeOH50-D samples (MeOH50-D CS, MeOH50-D SS, and MeOH50-D Al) compared with the initial distillation curve of MeOH50-D. The decrease in FBP of the MeOH50-D CrMo sample most likely occurred due to unstable conditions throughout the distillation process. The substance with the lowest boiling point evaporates first during distillation. Therefore, it is understandable that MeOH evaporates first from the MeOH50 blends, so the IBP values of MeOH50 blends correspond with the value of 100% methanol.

The observed variations in the research outcomes may also be due to the presence of contaminants, such as surface grease on the metal substrates. The metal bars in this study were not pretreated before immersion. Future similar immersion studies may consider proper cleaning of the metal surfaces. However, in this study the metals were left untreated in order to mirror real-life conditions. Untreated surfaces may sometimes yield the most significant results. Surface cleaning may remove segregated elements and existing surface contamination [43]. The surface of the metal rods can be cleaned with demineralized water, and degreased with ethanol and acetone [44].

These test results can show that, first, methanol, HVO, and HVOr exhibited relatively stable characteristics, regardless of contact with the metal rods. Second, the metals studied here were corrosion-resistant when immersed in HVO or MeOH50 or MeOH50–co-solvents fuel samples. However, it is important to note that the MeOH50 fuel, a blend of methanol and HVO without co-solvent, displayed relatively poor stability due to the occurrence of phase separation between methanol and HVO. Third, HVO and HVOr were compatible with the studied metals in the current experiment conditions, and this compatibility is critical to maintaining the integrity of fuel system components and preventing potential damage or corrosion. Fourth, the co-solvents 1-octanol and 1-dodecanol helped to form a stable, single-phase fuel of the methanol–HVO blend. Fifth, the slight leaching effect of aluminum and carbon steel in methanol may indicate methanol's corrosiveness in the

studied conditions. The experimental method to study especially methanol's corrosive effect could be developed further.

4.2. Effects of Trace Metals on Fuel Performance and Engines

Fuels derived from crude oil are known to possess relatively low concentrations of trace elements, typically measuring less than 1 ppm [30]. Both MeOH and HVO fuels in the present study had concentrations below 1 ppm for all the studied trace elements (Al, Cu, Si, Zn, Fe, Mn, V, and Pb). However, concentrations of Zn, Cu, Al, Mn, Pb, and Si exceeded the desired level of 1 ppm after the immersion test in some of the samples. Consequently, the discussion will now delve into the potential impact on engine performance and combustion of these detected elements with concentrations above 1 ppm.

Specific metals have a detrimental impact on combustion and engine operation, resulting in complications such as the formation of ash, deposition of undesirable sub-stances, and the clogging of filters. The metals identified in this regard include Na, Si, Ca, and Al. Of these, Na is particularly problematic due to its propensity to induce hot corrosion in engine components. Moreover, alkali metals like Na and K have the potential to adversely affect performance and efficiency of exhaust aftertreatment systems used for emissions control [29]. Si and Al in methanol and MeOH50 fuels may adversely affect combustion and engine operation, leading to problems such as ash formation, deposits, and filter-clogging.

Patel et al. [45] studied the use of biodiesel from waste cooking oil, jatropha, and karanja oil as a fuel, using ICP-OES to quantify the levels of trace metals present in the particulate matter emitted by engines. Their analysis revealed the presence of several trace metals, including Ca, Cu, K, Na, Zn, and Al. This indicates that trace metals (Cu, Zn, and Al) dissolved into methanol and MeOH50 fuels could have the potential to be released into particulate matter during the combustion process.

Research by Stepien and Krasodomski [46] confirmed that surpassing the 1 ppm threshold of Zn content in fuel, as stipulated in the CEC F-98-08 test procedure, results in a significant decline in the fuel's detergent properties. This decline led to the loss of maximum engine power. Notably, this effect occurs irrespective of the chemical structure of the Zn present in the fuel. The Zn content present in MeOH CS (2 ppm) fuel may have the potential to induce a reduction in the fuel´s detergent efficiency, and subsequently affect engine power.

A study by Joo and Suh [40] proposed that concentrations of Si exceeding 1.0 µg/mL are very high. The presence of Si in naphtha was identified as a contributing factor to the formation of silica deposits in spark plugs, catalytic converters, and oxygen sensors. These deposits are associated with adverse consequences, including degradation of fuel economy, elevated emissions, and the potential for catalytic converter damage. Remarkably, nine of the 28 tested samples (Table 3) in the current study exhibited detectable levels of Si above 1 ppm. Based on Joo and Suh's research conclusion, the increase in the trace element Si in these fuel samples may lead to detrimental effects, including a reduction in fuel economy, an increase in emissions, and the possibility of catalytic converter damage. SiO_2 from the ICP-OES torch may contaminate the samples and thus may be a factor in the measurement [37]. Thus, it is unclear whether the detected amount of Si in the studied samples is real and may actually affect fuel economy and emissions.

According to Patel et al. [45], trace metals emitted in particulates from diesel engines have significant environmental and health impacts. Exposure to Cu traces can induce sensations of cold, as well as mild nasal and eye discomfort, and irritation. Prolonged exposure to iron oxides over many years may lead to benign pneumoconiosis, also known as siderosis. Inhalation of substantial traces of Mn or its fumes can cause lung irritation and may lead to pneumonia. Inhalation of Zn traces can result in metal fume fever, characterized by symptoms such as fatigue, fever, and cough. Additionally, Pb is carcinogenic [45]. Trace amounts of Pb in all samples of MeOH50-O, MeOH50-D, and HVOr in the current study were less than 4 ppm, the determination level of the used method. However, exhaust emissions of fuel containing the heavy metal Pb cause air pollution and have potential im-

plications in lung cell damage, poisoning, anemia, neurotoxicity, and carcinogenesis [47,48]. Therefore, further studies should consider a more accurate method (having a lower determination limit) for analyzing Pb content, to ensure that its concentration does not exceed 1 ppm. Additionally, the transformation of trace metals to soot when using MeOH-HVO blends warrants detailed analysis in future studies. A study by Morajkar et al. [49] used high-resolution ICP-MS techniques to analyze the transmission of trace metals to PM in diesel and diesel/Karanja biodiesel blends.

5. Conclusions

This study investigated the corrosion and compatibility of methanol, HVO, HVOr, and MeOH-HVO fuel blends with and without co-solvents with selected metals: aluminum, carbon steel, stainless steel, and a special alloy (MoC210M/25CrMo4+SH). After immersion of the metal samples in the fuels at room temperature for 60 days, the corrosion and compatibility of the metals and fuels were evaluated by comparing the visual change of the surface of the metals, and by analyzing the content of trace metals (Al, Cu, Fe, Mn, Si, V, Zn, and Pb) in the fuel samples. Additionally, density, kinematic viscosity, and distillation properties of the fuels were analyzed before and after the metals were immersed in the fuels.

The results of this study lead to the following conclusions:

- A blend of methanol and HVO/HVOr displays relatively poor stability due to the occurrence of phase separation between methanol and HVO/HVOr. The co-solvents 1-octanol and 1-dodecanol can be used to form stable, single-phase methanol–HVOr fuel blends.
- Visual assessment showed that methanol, HVO, HVOr, MeOH50, MeOH50-1-octanol, and the MeOH50-1-dodecanol fuel blends did not induce observable corrosion on the metallic surfaces.
- The metals were corrosion-resistant when immersed in HVO and MeOH 50 fuel samples in the studied conditions. Methanol had a slight dissolving effect on aluminum (dissolving Al) and carbon steel (dissolving Zn).
- The trace metal concentrations in MeOH50-O, MeOH50-D, and HVOr fuels did not change after metal immersion. These three fuels did not dissolve metal in the studied conditions.
- Methanol, HVO, and HVOr exhibited relatively stable characteristics when in contact with metals. The immersion of selected metals into the fuels had no impact on the density of methanol, HVO, HVOr, MeOH50, MeOH50-1-octanol, and MeOH50-1-dodecanol fuels. Moreover, the immersion did not influence kinematic viscosity and distillation behavior of methanol, HVO, and HVOr fuels.
- An experimental method needs to be developed further to study the corrosive effect of methanol in particular, and to prove and secure different metals' resistance to corrosion.

Author Contributions: Conceptualization: H.W.-A. and K.S.; methodology: H.W.-A. and K.S.; investigation: H.W.-A. and K.S.; resources: K.S.; data curation: H.W.-A.; writing—original draft preparation: H.W.-A. and K.S.; writing—review and editing: H.W.-A., K.S., J.K. and C.N.; visualization: H.W.-A.; supervision: K.S., M.M. and S.N.; project administration: M.M.; funding acquisition: K.S., M.M. and S.N. All authors have read and agreed to the published version of the manuscript.

Funding: The work was conducted in the framework of the Flexible Clean Propulsion Technologies project with financial support from Business Finland (ref. 1310/31/2023).

Data Availability Statement: Data is contained within the article.

Conflicts of Interest: The authors declare no conflicts of interest.

References

1. Verhelst, S.; Turner, J.W.; Sileghem, L.; Vancoillie, J. Methanol as a Fuel for Internal Combustion Engines. *Prog. Energy Combust. Sci.* **2019**, *70*, 43–88. [CrossRef]
2. Anand, K.; Ra, Y.; Reitz, R.D.; Bunting, B. Surrogate Model Development for Fuels for Advanced Combustion Engines. *Energy Fuels* **2011**, *25*, 1474–1484. [CrossRef]
3. Liu, J.; Wu, P.; Ji, Q.; Sun, P.; Wang, P.; Meng, Z.; Ma, H. Experimental Study on Effects of Pilot Injection Strategy on Combustion and Emission Characteristics of Diesel/Methanol Dual-Fuel Engine under Low Load. *Energy* **2022**, *247*, 123464. [CrossRef]
4. No, S.Y. Application of Biobutanol in Advanced CI Engines—A Review. *Fuel* **2016**, *183*, 641–658. [CrossRef]
5. Szeto, W.; Leung, D.Y.C. Is Hydrotreated Vegetable Oil a Superior Substitute for Fossil Diesel? A Comprehensive Review on Physicochemical Properties, Engine Performance and Emissions. *Fuel* **2022**, *327*, 125065. [CrossRef]
6. Halada Nandhakrishnan, M.; Prashant Thakare, S. Alcoholate Corrosion of Ferrous Metals in Methanol-Gasoline Fuel Blends. *J. Chem. Technol. Metall.* **2020**, *55*, 2187.
7. Domínguez, V.M.; Hernández, J.J.; Ramos, Á.; Giménez, B.; Rodríguez-Fernández, J. Exploring the Effect of Methanol and Ethanol on the Overall Performance and Substitution Window of a Dual-Fuel Compression-Ignition Engine Fueled with HVO. *Fuel* **2024**, *359*, 130529. [CrossRef]
8. Liu, M. *Methanol as a Marine Fuel-Availability and Pre-Trial Considerations*; Nanyang Technological University: Singapore, 2020. Available online: https://www.ntu.edu.sg/docs/librariesprovider79/publication/mesd-webinar-2020-methanol-as-a-marine-fuel.pdf (accessed on 12 January 2024).
9. Wissner, N.; Healy, S.; Cames, M.; Sutter, J. *Methanol as a Marine Fuel*; Naturschutzbund Deutschland: Stuttgart, Germany, 2023.
10. Hunicz, J.; Mikulski, M.; Shukla, P.C.; Gęca, M.S. Partially Premixed Combustion of Hydrotreated Vegetable Oil in a Diesel Engine: Sensitivity to Boost and Exhaust Gas Recirculation. *Fuel* **2022**, *307*, 121910. [CrossRef]
11. Niemi, S.; Vauhkonen, V.; Mannonen, S.; Ovaska, T.; Nilsson, O.; Sirviö, K.; Heikkilä, S.; Kiijärvi, J. Effects of Wood-Based Renewable Diesel Fuel Blends on the Performance and Emissions of a Non-Road Diesel Engine. *Fuel* **2016**, *186*, 1–10. [CrossRef]
12. Spoof-Tuomi, K.; Vauhkonen, V.; Niemi, S.; Ovaska, T.; Lehtonen, V.; Heikkilä, S.; Nilsson, O. *Effects of Crude Tall Oil Based Renewable Diesel on the Performance and Emissions of a Non-Road Diesel Engine*; SAE Technical Papers; SAE International: Warrendale, PA, USA, 2021.
13. Ciniviz, M.; Köse, H.; Canli, E.; Solmaz, Ö. An Experimental Investigation on Effects of Methanol Blended Diesel Fuels to Engine Performance and Emissions of a Diesel Engine. *Sci. Res. Essays* **2011**, *6*, 3189–3199. [CrossRef]
14. Duan, Q.; Yin, X.; Wang, X.; Kou, H.; Zeng, K. Experimental Study of Knock Combustion and Direct Injection on Knock Suppression in a High Compression Ratio Methanol Engine. *Fuel* **2022**, *311*, 122505. [CrossRef]
15. Hunicz, J.; Matijošius, J.; Rimkus, A.; Kilikevičius, A.; Kordos, P.; Mikulski, M. Efficient Hydrotreated Vegetable Oil Combustion under Partially Premixed Conditions with Heavy Exhaust Gas Recirculation. *Fuel* **2020**, *268*, 117350. [CrossRef]
16. Wang-Alho, H.; Sirviö, K.; Balogun, F.; Kaivosoja, J.; Nuortila, C.; Mikulski, M.; Niemi, S. Properties of Chemically Stabilized Methanol-HVO Blends. *Agron. Res.* **2024**, *22*. [CrossRef]
17. Hoang, A.T.; Tabatabaei, M.; Aghbashlo, M. A Review of the Effect of Biodiesel on the Corrosion Behavior of Metals/Alloys in Diesel Engines. *Energy Sources Part A Recovery Util. Environ. Eff.* **2020**, *42*, 2923–2943. [CrossRef]
18. Wang-Alho, H.; Sirviö, K.; Hissa, M.; Mikulski, M.; Niemi, S. Methanol-HVO Blends for Efficient Low-Temperature Combustion: Analytical Research on Fuel Properties. *Agron. Res.* **2023**, *21*, 994–1005. [CrossRef]
19. Sathish Kumar, T.; Ashok, B. Material Compatibility of SI Engine Components towards Corrosive Effects on Methanol-Gasoline Blends for Flex Fuel Applications. *Mater. Chem. Phys.* **2023**, *296*, 127344. [CrossRef]
20. Surisetty, V.R.; Dalai, A.K.; Kozinski, J. Alcohols as Alternative Fuels: An Overview. *Appl. Catal. A Gen.* **2011**, *404*, 1–11. [CrossRef]
21. Martin, A.; O'malley, J. *Compatibility of Methanol Fuel Blends with Gasoline Vehicles and Engines in Indonesia*; The International Council on Clean Transportation: Washington, DC, USA, 2021.
22. Muthuraman, V.S.; Patel, A.; Shreya, V.; Vaidyanathan, A.; Reshwanth, K.N.G.L.; Karthick, C.; Jacqueline, P.J.; Jan Gęca, M.; Ashok, B.; Sivagami, K.; et al. Progress on Compatibility Issues of Alcohols on Automotive Materials: Kinetics, Challenges and Future Prospects—A Comprehensive Review. *Process Saf. Environ. Prot.* **2022**, *162*, 463–493. [CrossRef]
23. Gao, Z.; Wu, S.; Luo, J.; Zhang, B.; Zhang, H.; Xiao, R. Optimize the Co-Solvent for Methanol in Diesel with Group of Oxygen-Containing Reagents: Molecular Structure and Intermolecular Forces Analysis. *Fuel Process. Technol.* **2021**, *222*, 106980. [CrossRef]
24. Yilmaz, N.; Atmanli, A.; Vigil, F.M. Quaternary Blends of Diesel, Biodiesel, Higher Alcohols and Vegetable Oil in a Compression Ignition Engine. *Fuel* **2018**, *212*, 462–469. [CrossRef]
25. Rajesh Kumar, B.; Saravanan, S. Use of Higher Alcohol Biofuels in Diesel Engines: A Review. *Renew. Sustain. Energy Rev.* **2016**, *60*, 84–115. [CrossRef]
26. Shahabuddin, M.; Mofijur, M.; Shuvho, M.B.A.; Chowdhury, M.A.K.; Kalam, M.A.; Masjuki, H.H.; Chowdhury, M.A. A Study on the Corrosion Characteristics of Internal Combustion Engine Materials in Second-Generation Jatropha Curcas Biodiesel. *Energies* **2021**, *14*, 4352. [CrossRef]
27. Nam Cao Ho Chi, D.; Dao Nam, C.; Anh Tuan Ho Chi, H. The 11th Seatuc Symposium Impact of Coconut Oil Acid Component on Fuel System Materials Durability and Corrosion in Diesel Engines. In Proceedings of the SEATUC, Nakhon Ratchasima, Thailand, 23–24 February 2022.

28. Liu, Z.; Guo, Z.; Rao, X.; Xu, Y.; Sheng, C.; Yuan, C. A Comprehensive Review on the Material Performance Affected by Gaseous Alternative Fuels in Internal Combustion Engines. *Eng. Fail. Anal.* **2022**, *139*, 106507. [CrossRef]
29. Worldwide Fuel Charter Committee. Biodiesel Guidelines. 2009. Available online: https://www.acea.auto/uploads/publications/20090423_B100_Guideline.pdf (accessed on 12 January 2024).
30. Mdluli, N.S.; Nomngongo, P.N.; Mketo, N. A Critical Review on Application of Extraction Methods Prior to Spectrometric Determination of Trace-Metals in Oily Matrices. *Crit. Rev. Anal. Chem.* **2022**, *52*, 1–18. [CrossRef]
31. Neste Corporation. Neste Renewable Diesel Handbook. 2020. Available online: https://www.sustainable-ships.org/stories/2023/neste-renewable-diesel-handbook (accessed on 12 January 2024).
32. Lampinen, A. *Uusiutuvan Liikenne-Energian Tiekartta*; Karelia University of Applied Sciences: Joensuu, Finland, 2009; ISBN 9789516041004. Available online: https://www.theseus.fi/handle/10024/127014 (accessed on 12 January 2024). (In Finnish)
33. Metallinjalostajat, R. *Teräskirja*, 9th ed.; Bookwell Oy: Helsinki, Finland, 2014. (In Finnish)
34. *EN 14538*; Fat and Oil Derivatives—Fatty Acid Methyl Ester (FAME)—Determination of Ca, K, Mg and Na Content by Optical Emission Spectral Analysis with Inductively Coupled Plasma (ICP OES). European Committee for Standardization: Brussels, Belgium, 2006.
35. *EN 14107*; Fat and Oil Derivatives—Fatty Acid Methyl Esters (FAME)—Determination of Phosphorus Content by Inductively Coupled Plasma (ICP) Emission Spectrometry. European Committee for Standardization: Brussels, Belgium, 2003.
36. *ASTM D7042-21a*; Standard Test Method for Dynamic Viscosity and Density of Liquids by Stabinger Viscometer (and the Calculation of Kinematic Viscosity). ASTM International: West Conshohocken, PA, USA, 2021.
37. Novotny-Farkas, F.; Böhme, W.; Stabinger, H.; Belitsch, W. Customer Portrait. In *The Stabinger Viscometer: A New and Unique Instrument for Oil Service Laboratories*; Anton Paar: Vienna, Austria, 2010; p. 4.
38. *ASTM D7345-17*; Standard Test Method for Distillation of Petroleum Products and Liquid Fuels at Atmospheric Pressure (Micro Distillation Method). ASTM International: West Conshohocken, PA, USA, 2024.
39. Kalghatgi, G.; Kalghatgi, G. *FuelEngine Interactions*; SAE International: Warrendale, PA, USA, 2014; p. 255.
40. Joo, S.; Suh, D. Facile and Precise Quantitative Determination of Silicon in Naphtha by Inductively Coupled Plasma-Optical Emission Spectroscopy. *J. Anal. Sci. Technol.* **2022**, *13*, 30. [CrossRef]
41. Yahya, S.I.; Aghel, B. Estimation of Kinematic Viscosity of Biodiesel-Diesel Blends: Comparison among Accuracy of Intelligent and Empirical Paradigms. *Renew. Energy* **2021**, *177*, 318–326. [CrossRef]
42. Vallinayagam, R.; Vedharaj, S.; Yang, W.M.; Roberts, W.L.; Dibble, R.W. Feasibility of Using Less Viscous and Lower Cetane (LVLC) Fuels in a Diesel Engine: A Review. *Renew. Sustain. Energy Rev.* **2015**, *51*, 1166–1190. [CrossRef]
43. *ASTM G31-72(2004)*; Standard Practice for Laboratory Immersion Corrosion Testing of Metals. ASTM International: West Conshohocken, PA, USA, 2012.
44. Matějovský, L.; Macák, J.; Pospíšil, M.; Baroš, P.; Staš, M.; Krausová, A. Study of Corrosion of Metallic Materials in Ethanol-Gasoline Blends: Application of Electrochemical Methods. *Energy Fuels* **2017**, *31*, 10880–10889. [CrossRef]
45. Patel, C.; Chandra, K.; Hwang, J.; Agarwal, R.A.; Gupta, N.; Bae, C.; Gupta, T.; Agarwal, A.K. Comparative Compression Ignition Engine Performance, Combustion, and Emission Characteristics, and Trace Metals in Particulates from Waste Cooking Oil, Jatropha and Karanja Oil Derived Biodiesels. *Fuel* **2019**, *236*, 1366–1376. [CrossRef]
46. Stepien, Z.; Krasodomski, W. Effect of Trace Zinc Amounts Introduced in Various Chemical Structures in Diesel Fuel on Coke Deposits of Fuel Injectors of a CI Engine. *Int. J. Eng. Res.* **2020**, *21*, 755–765. [CrossRef]
47. Wen, J.; Wang, X.; Zhang, Y.; Zhu, H.; Chen, Q.; Tian, Y.; Shi, X.; Shi, G.; Feng, Y. PM2.5 Source Profiles and Relative Heavy Metal Risk of Ship Emissions: Source Samples from Diverse Ships, Engines, and Navigation Processes. *Atmos. Environ.* **2018**, *191*, 55–63. [CrossRef]
48. Fang, W.; Yang, Y.; Xu, Z. PM10 and PM2.5 and Health Risk Assessment for Heavy Metals in a Typical Factory for Cathode Ray Tube Television Recycling. *Environ. Sci. Technol.* **2013**, *47*, 12469–12476. [CrossRef] [PubMed]
49. Morajkar, P.P.; Abdrabou, M.K.; Raj, A.; Elkadi, M.; Stephen, S.; Ibrahim Ali, M. Transmission of Trace Metals from Fuels to Soot Particles: An ICP-MS and Soot Nanostructural Disorder Study Using Diesel and Diesel/Karanja Biodiesel Blend. *Fuel* **2020**, *280*, 118631. [CrossRef]